Conversion of CO_2 by non-thermal inductively-coupled plasma catalysis

Edwin Devid*[a], Maria Ronda-Lloret[b], Qiang Huang[a,c], Gadi Rothenberg[b], N. Raveendran Shiju[b], Aart Kleyn*[a]

[a] dr. E. J. Devid, dr. Q. Huang, Prof. dr. A. W. Kleyn
Center of Interface Dynamics for Sustainability
Institute of Materials, China Academy of Engineering Physics
596 Yinhe Road 7th section, Chengdu, Sichuan 610200, People's Republic of China
E-mail: ejdevid@outlook.com ; a.w.kleijn@contact.uva.nl

[b] M. Ronda-Lloret MSc., Prof. dr. G. Rothenberg, dr. N. Raveendran Shiju
Van 't Hoff Institute for Molecular Sciences
Faculty of Science, University of Amsterdam
P.O. Box 94157, 1090 GD Amsterdam, The Netherlands

[c] Dr. Q. Huang
School of Optoelectronic Engineering
Chongqing University of Posts and Telecommunications
Chongqing 400065, People's Republic of China

Abstract:

CO_2 decomposition is a very strongly endothermic reaction where very high temperatures are required to thermally dissociate CO_2.
Radio frequency inductively-coupled plasma enables to selectively activate and dissociate CO_2 at room temperature.
Tuning the flow rate and the frequency of the radio frequency inductively-coupled plasma gives high yields of CO under mild conditions.
Finally the discovery of a plasma catalytic effect has been demonstrated for CO_2 dissociation that shows a significant increase of the CO yield by metallic meshes. The metallic meshes become catalyst under exposure to plasma to activate the recombination reaction of atomic O to yield O_2, thereby is reducing the reaction to convert CO back to CO_2.
Inductively-coupled hybrid plasma catalysis allows access to study and to utilize high CO_2 conversion in a non-thermal plasma regime. This advance offers opportunities to investigate the possibility to use radio frequency inductively-coupled plasma to store superfluous renewable electricity into high-valuable CO in times where the price of renewable electricity is plunging.

Keywords: CO_2, RF-ICP, plasma reactor, conversion, metal mesh, QMS, XPS, XRD, SEM.

I. INTRODUCTION

Can catalysis solve our CO_2 problem? This interesting question was discussed in the magazine *Chemistry World* of July 2019. Recent publications about CO_2 splitting through thermal (catalytic) reactors support our findings that up to now it is still very difficult to reduce CO_2, due to its high thermodynamic stability [1-3]. Very high temperatures > 2000 K are required to thermally split CO_2 into $CO + ½O_2$ and obtain a CO_2 conversion of 1.5% [4] (reaction 1).

$CO_2 \leftrightarrow CO + ½ O_2$ ($\Delta H° = +283$ kJ/mol or 2.9 eV/mol) (1)

Even with the presence of a suitable catalyst a temperature of >1000 K is required to obtain reasonable decomposition rates for CO_2 splitting [1].
In order to counter the effects of greenhouse gases on our environment [5-7], sustainable solutions are needed to safeguard both our planet biodiversity and the urgent global requirement of both energy and raw materials in the current 21st century [4, 8-10]. Now we have arrived at a point where we need to stop emitting CO_2 and other greenhouse gases and research challenging alternative ways in order to replace our traditional methods of producing chemicals and energy materials from fossil fuels.
A promising alternative is the use of plasma technology [4, 11-15] where greenhouse gases and simple hydrocarbons can be converted into high-value chemicals and solar fuels (i.e. solar fuels refer to producing fuel from energy that has been derived from sustainable sources like sun, wind, etc.). Research in this scientific field has revealed great potential and progress into using plasma technology to enable endothermic chemical reactions at low reactor temperatures, to improve the properties of catalysts and to synthesize renewable energy materials from greenhouse gases [4, 13 14]. So far different types of plasma technology [16-26] with or without catalysts have been tested on their performance compared to the traditionally thermal chemical processes. Especially a lot of work has been done on Dielectric Barrier Discharge (DBD) generated plasma to dissociate CO_2. While DBD offers a few advantages in simple construction and application, the presence of catalyst and/or, addition of carrier gas (i.e. Ar) and tuning carefully the process conditions (i.e. flow rate, particle size packing materials, etc.) are required to reach conversions and energy efficiencies in the range of 30-45% and 5-10% respectively [4, 27, 28].
The research on plasma exposed materials and plasma driven chemical processes is still novel and unexplored. Especially plasma driven processes by radio frequency inductively-coupled plasma (RF-ICP) are currently unexplored and exhibit a lot of potential [4].
The role of catalysis for CO_2 conversion by using RF-ICP requires further study. This can team up with studies into the reactions on catalytic surfaces that are actively studied theoretically. These theoretical studies also aim to make a connection to CO_2 conversion by electrochemical ways, see for instance [29, 30]. A very different catalytic approach is to use the Boudouard reaction to enhance the CO yield [31]. Both enhanced theory and the Boudouard reaction have not yet been applied to RF-ICP conversion.
To improve the yield of CO during CO_2 splitting in RF-ICP the role of atomic O and O_2 deserves further study due to their involvement with the back reaction of CO toward CO_2. Atomic O that is produced by reaction 1 is expected to bounce/reflect by the quartz reactor

tube. Because the silicon oxide surface is highly saturated by bound O atoms with a strong electron negativity. It is therefore probable that at the quartz surface no recombination of atomic O atoms or dissociation of O_2 takes place.
Based on the CO_2 splitting reaction (see reaction 1) the flow of CO can be twice as much versus the O_2 flow. This fact is observed during CO_2 splitting experiments where the pressure in the plasma reactor increases by applying more input power. In many cases we have observed that the CO/O_2 ratio increases to a factor of 3. This change can possibly be elaborated via the reaction kinetic of CO_2 splitting. O_2 is generated by the reaction [32]:

$CO_2 + M \rightarrow CO + O + M$ (reaction rate: 10^{-7} cm^3/s) (2)

Followed by the reaction:

$CO_2 + O \rightarrow CO + O_2$ (reaction rate: 10^{-12} cm^3/s) (3)

Reaction 2 is faster than reaction 3, this gives atomic O the possibility to initiate the reverse reaction $CO + O \rightarrow CO_2$.

The dissociation reaction of O_2 [32] will also occur in the RF-ICP:

$O_2 + M \rightarrow M + O + O$ (reaction rate: 10^{-8} cm^3/s) (4)

The recombination of atomic O and dissociation of O_2 are presumably nearly equally fast, this enables the possibility that reaction 2 can produce faster CO directly followed by recombination of atomic O to O_2. This will prevent that atomic O is available to initiate the back reaction..
So with the presence of at third body (i.e. like a metal mesh) reaction 2 has preference. The binding energy of O to metal oxide or hydrocarbons contaminations on the system walls is expected to be higher than to silicon oxide. This in turn enables an increase of CO/O_2 ratio beyond 2 due to adsorption of atomic O atoms to the system walls. It should be noted that there are long bellows between the exit of the plasma reactor and entrance to the QMS.
Any amount of C formed during the CO_2 splitting will presumably stick to the reactor wall and will not participate in the reaction of $C + O_2 \rightarrow CO_2$.
RF-ICP allows to activate CO_2 through stepwise vibrational excitation where CO_2 will be split into $CO + ½O_2$ at ambient temperatures. So far no record has been mentioned to perform CO_2 splitting with a catalyst in RF plasma. only Spencer and Gallimore [33] have performed CO_2 splitting in a microwave plasma reactor with a catalyst.. In their case the addition of a catalyst decreased the CO yield.
Previously work from Spencer et al. [32, 34] showed that CO_2 splitting via 13.56 MHz RF power source can reach CO_2 conversions of 90% at 15 sccm CO_2 and 1000 W (i.e. > 1000 eV/mol). Due to the low feed rate and very high power usage the energy efficiency will in turn be not higher than 3%.
Scientists in surface science have done extensive research on the chemical and physical properties of CO_2 and its interaction with various types of metals and metal oxides for both fundamental and applicational purposes (i.e. the use of Zn, Cu, etc. for catalytic reaction)[35-39].
This work will investigate multiple experimental conditions in order to discover unknown effects and features about CO_2 splitting. The knowledge and findings obtained from these CO_2 splitting experiments allow us to answer the question on how CO_2 splitting proceeds

under mild conditions (i.e. low pressures and powers) and how these experimental parameters will affect the conversion of CO_2.
The main question we want to solve in this work is: is there a catalytic effect when combining a third body (metallic mesh) and RF-ICP plasma during CO_2 splitting?

II. EXPERIMENTS

All experiments were carried out in a designated RF-ICP reactor constructed in-house (see FIG. 1). The plasma reactor consists of a quartz tube, with a diameter of 40 mm and length of 600 mm. It is supported by two stainless steel flanges and sealed by O-rings. The reactor tube is surrounded by a water-cooled copper coil. To establish efficient coupling of RF energy into the plasma, a matching box is kept between the RF power supply and the copper coil.
A detailed technical description of the setup is published elsewhere [34, 40, 41].
In this work two types of RF power supplies (13.56 MHz, 2 kW and 27,12 MHz, 4kW) have been used to test the influence of RF frequency on CO_2 splitting by RF plasma.
The 13.56 MHz RF power was provided by a water cooled RF power generator with RF output of 2000 W from Rishige Electronics Technology.
The 27,12 MHz RF power was provided by a water cooled RF power generator with RF output of 4000 W, (~700 V) from Advance Energy.
The maximum power used was 350 W and the reflected power was kept between 1 till 4 W (dependent on applied input power) by the matching box. The gases used in the reaction were directly obtained from gas cylinders and mixed before going into the reactor. Each gas cylinder was equipped with calibrated mass flow controllers (MFC, Sevenstar D07-19B) to set the flow. The plasma ignited inside the reactor tube, after supplying RF power. Prior to feeding the reaction gases, the reactor was evacuated to 1 Pa by a rotary pump with the nominal pumping speed around 18 L/s.
The composition of the gaseous products from the plasma reactor was determined by quadrupole mass spectrometry (QMS). QMS allows us to observe in real time the species formed in the plasma at low pressures in a way similar to ref. [42]. In this way the state of the plasma was checked continuously.
A catalyst holder is a quartz tube that can keep any metal meshes perpendicular positioned versus the plasma beam. The space between the metal meshes inside the catalyst holder is called a catalyst bed (see FIG. S1). The RF-ICP can be opened so that the catalyst can be inserted inside the reactor.
The chemical composition of the catalyst was determined by X-ray photo-electron spectroscopy (XPS). The binding energies were referred to the C1s peak at 284.8 eV to compensate for surface charging effects.
X-Ray diffraction (XRD) patterns were recorded on a MiniFlex II diffractometer using Cu Kα radiation. The X-ray tube was operated at 30 kV and 15 mA. Measurements were recorded at an angle (2θ) range of 10-90° with a turning speed of 2.5 °·min^{-1}.
Thermal CO_2 splitting reactions were performed under atmospheric pressure in a six-flow parallel reactor system. This system is a modernized version of the classic six flow system described by Pérez-Ramírez et al. It consists of six individual fixed-bed quartz reactors located in a furnace [43, 44] . Here, a flow of 10 ml/min of CO_2 diluted in Ar (80% Ar, 20% CO2) was passed through the reactor with 0.3 g of Cu mesh at 900 °C for 2 h.
The thermal oxidation of a Cu mesh was performed in a tubular furnace, using a flow of 50 mL/min of compressed air at 400 °C for 1 h.
Scanning Electron Microscopy (SEM) images were recorded with a FEI Verios 460.

Elemental analysis was performed with Energy Dispersive Spectroscopy (EDS) in a Oxford Xmax 80 mm^2 Silicon Drift Detector.

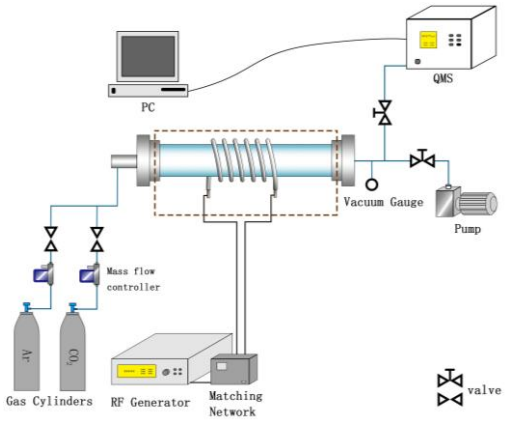

FIG. 1 Schematic diagram of experimental setup to do CO_2 splitting in non-thermal RF plasma.

III. RESULTS AND DISCUSSION

RF-ICP driven CO_2 splitting enables CO_2 dissociation through vibrational activation (i.e. "selective excitation") of one degree of freedom [40]. The vibrationally excited CO_2 will further interact with each other or collide with the plasma electrons, leading to a successive "vibrational pumping" up along the vibrational levels. This co-called ladder climbing effect will result that the vibrationally excited CO_2 molecules reach the energies of dissociation at low gas temperatures.

To study the CO_2 splitting process we have used the following expressions. The specific energy input (SEI) is described in equation 1 and represents a key factor to determine the conversion and energy efficiency during CO_2 splitting in RF-ICP. The SEI together with the CO_2 conversion, χ gives a factor called the energy efficiency, η (see equation 2) that shows how efficient the CO_2 splitting in a "cold" non thermal plasma goes compared to the standard reaction enthalpy.

$$\mathbf{SEI}\ \ [\mathbf{eV/molecule}] = \frac{\mathbf{Power}\ \ [\mathbf{kW}]\ \ 6.24\times10^{21}[\mathbf{eV/kJ}]\ \ 24.5\ \ [\mathbf{L/mol}]\ \ 60\ \ [\mathbf{s/min}]}{\mathbf{Flowrate}\ \ [\mathbf{L/min.}]\ \ 6.022\times10^{23}[\mathbf{molecule/mol}]} \quad (1)$$

$$\eta = \frac{\chi_{\mathbf{total}}\ \ \Delta\mathbf{H}^{\circ}_{\mathbf{298K}}[\mathbf{eV/molecule}]}{\mathbf{SEI}\ \ [\mathbf{eV/molecule}]} \quad (2)$$

1. The effect of the RF frequency, flow and air plasma pretreatment on CO_2 splitting

The performance of CO_2 splitting by RF-ICP can be tuned through different parameters. FIG. S2 shows the dependence of the CO_2 splitting process on the RF frequency. The black line shows that generating RF plasma with 13.56 MHz power generator lets the conversion increase with power to 36% (300 W). When doubling the frequency with a 27.12 MHz power generator, a plasma is generated that gives higher conversions (i.e. 46% at 300 W) as function of the power. Generating RF-ICP at higher frequencies (>100 MHz) opens the possibility to reach very high CO_2 conversion (toward 90% projected on applying > 600 MHz of RF power) under non-thermal plasma conditions. By increasing the CO_2 conversion in RF-ICP thereby advantageously will be further increased the energy efficiency while not subjecting the current CO_2 splitting process to dominate vibrational–translational (V-T) relaxation, which has a detrimental effect on the energy efficiency in thermal plasmas [11]. This makes CO_2 splitting on an industrial scale through RF-ICP viable [4]. In fact, such efficiencies are not quite reached at about 2.45 GHz, using microwave excitation [34].
The conversion of CO_2 into CO can be further increased with 5%-8% by performing a pretreatment step prior of the start of CO_2 splitting by RF-ICP (see FIG. S3). This step involves letting air plasma flow inside the empty straight quartz reactor tube. 200 sccm air is ignited into plasma and kept at 200 W during the pretreatment period of 45 min till 60 min. The effect of this pretreatment is first that the quartz reactor tube will be cleaned from any visible or invisible carbon layer on the quartz material. This will improve the vacuum conduction inside the quartz plasma reactor tube. The pressure in the RF-ICP reactor will be lower and this improves the CO_2 splitting process.
Furthermore we have experienced that the CO_2 flow rate has a large influence on the conversion. Very high yields of CO will be obtained under mild conditions by tuning the specific energy input (SEI) (see FIG. S4).

2. Plasma catalysis of CO_2 splitting through metal meshes

Here we studied the effects of several metals and metal oxides to investigate their possible plasma catalytic effects by RF-ICP.
In order to insert a metal into our RF-ICP driven reactor we have developed two concepts to optimize the interaction of a metal surface with the CO_2 plasma.
The first concept that is tested to study the influence of metal surface and metal oxides is done through use of a catalyst holder (see FIG. S1).
FIG. 2 shows the performance of CO_2 splitting by a catalyst holder equipped with brass meshes in the RF-ICP reactor.

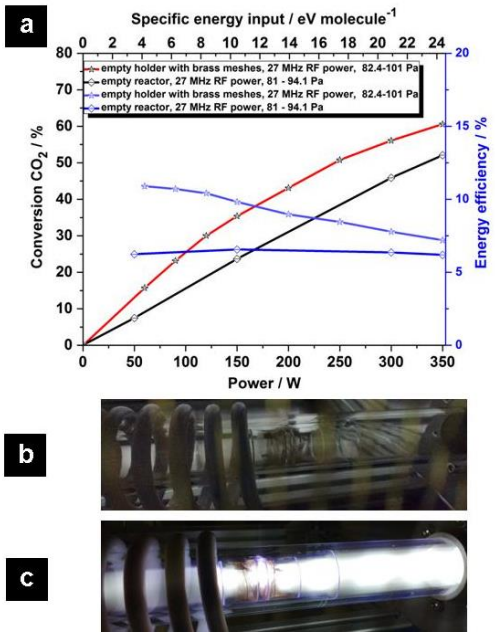

FIG. 2(a) The CO_2 conversion and energy efficiency as function of the input power and SEI. Black line is reference conversion of an empty RF-ICP reactor. Red line is the conversion obtained via the catalyst holder equipped with brass meshes.
(b) CO_2 flowing through the RF-ICP reactor while the input power is off (0 W).
(c) CO_2 ignited in plasma and percolating through the brass mesh inside the catalyst holder (input power is 90 W with a pressure of 95.5 Pa (on all images the feed gas flows from left to right).
Reaction condition: 200 sccm CO_2.

FIG. 2a shows that the conversion of CO_2 in the presence of a catalyst holder containing brass meshes significantly increases. Here the absolute CO_2 conversion increases with 10% at 300 W. Furthermore the energy efficiency increases especially at lower input powers. After CO_2 splitting, the plasma exposed brass meshes have a darker blue coloured surface. Fresh metal meshes before plasma exposure have a red/orange, goldlike or silver/metallic surface colour at respectively copper, brass and stainless steel coloured meshes.
This indicates a change to the metal oxide surface layer on the brass meshes. The mass of the brass meshes used before and after CO_2 splitting show no significant change.
There are three possible ways for CO_2 to dissociate:
1. Through direct electronic excitation CO2 can be splitted into CO and O, but this requires impacts by highly energized electrons (>11 eV).
2. The vibrational energy level is step wise increased until the CO_2 molecule splits into CO and O.
3. The CO_2 molecule gains an increase of vibrational energy, but has not reached the energies that allow the CO_2 molecule to spontaneous dissociate. Instead the partially vibrationally excited CO_2 molecule comes in contact with a metal oxide surface where it will stick. Since sticking of the partially excited CO_2 molecule possess fluctuations in binding energy upon contact with the metal oxide. It seems logical that the bonds of vibrationally excite CO_2 will

change and dump first the CO part from the metal oxide surface followed later by the release of the atomic O from the metal oxide surface when hit by another atomic O.
The brass metal meshes in the catalyst holder appear to stimulate the recombination of atomic O into O_2. The atomic O generated from reaction 1 here make contact with the oxidized metal mesh. The atomic O binds to the oxidized surface of the metal mesh. Eventually the oxidation of the metal mesh surface takes place, but is finite because the oxide thickness on metal surfaces get saturated in time [45, 46]. The oxidized metal mesh (i.e. change of surface colour) exhibits a change to the metal oxide surface thereby weakening the O atom bond with the metal oxide. This will result that from the plasma exposed metal surface O_2 can escape thereby reducing further the back reaction of CO into CO_2 assuming that reaction 2 is faster than reaction 4.
The presence of the brass metal mesh inside a RF-ICP driven CO_2 splitting process demonstrates for the first time a catalytic effect. In addition we have performed at the University of Amsterdam CO_2 splitting in a thermal catalytic reactor containing a similar piece of brass metal mesh. Here, at a maximum of 900 °C the thermal catalytic reactor showed no conversion of CO_2 into CO as mentioned earlier [1, 3, 4].
From these findings we conclude that the fact that a catalyst works in a plasma catalytic reactor does not automatically works in a thermal catalytic reactor that the plasma-catalytic reaction is driven and vice versa.. This also indicates that the catalyst in the plasma case is driven by the enhancement of the recombination reaction $O + O \rightarrow O_2$, which cannot run in the thermal reactor, because there is no significant O-atom concentration. Catalytic dissociation of CO_2 on the Cu catalyst would not run in a thermal reactor as it is unable to excite the CO_2 vibrationally. We should note that in the plasma reactor the CO_2 may be vibrationally excited and certain materials might become more catalytically active.
The second concept that is used to test the properties of metal surfaces on the CO_2 splitting process is done through use of a metal mesh capsule (see FIG. 3) in order to let the CO_2 plasma interact and percolate through the metal meshes.

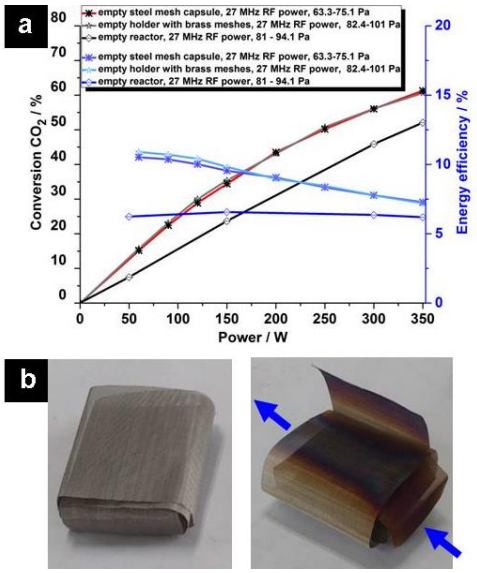

FIG. 3 (a) The CO_2 conversion and energy efficiency as function of the input power. Black line is reference conversion of an empty RF-ICP reactor. Red line is the conversion obtained

via one stainless steel mesh capsule. The grey line is for comparison the CO_2 splitting performance of using a catalyst holder containing brass meshes (see also FIG. 2)
(b) A image of a fresh stainless steel mesh capsule (left side). A image of a CO_2 plasma exposed stainless steel mesh capsule (right side) after going stepwise from 0 - 350 W in 106 minutes. The blue arrows shows the direction of the CO_2 plasma flow over and through the mesh capsule.
Reaction conditions: 200 sccm CO_2. For the experiment with using one stainless steel mesh capsule an additional second vacuum pump (located at the side toward the QMS) is used to lower a bit the starting pressure (with 5 till 7 Pa) before the plasma driven CO_2 splitting is started.

FIG. 3a shows that, besides a catalyst holder equipped with brass meshes, a stainless steel mesh capsule also gives a significant increase in the absolute CO_2 conversion. Both conceptual approaches (i.e. metal meshes) give similar performances on CO_2 conversion and energy efficiency. In the experimentation with one stainless steel mesh capsule an additional second vacuum pump was used to increase the pump speed and slightly lower the starting pressure (i.e. 5 till 7 Pa) before CO_2 splitting. From earlier research (i.e. [40]) was learned that lower the pressure in a RF-ICP reactor can be beneficial to further increase the CO yield during CO_2 splitting. FIG 3a shows that the presence of a metal mesh under higher pumping speed in the RF-ICP has a significant effect on the conversion of CO_2. The additional second vacuum pump connected in parallel to the plasma reactor allows to increase the pumping speed with a factor of >2 inside the RF-ICP reactor. Under these conditions the converted CO_2 by a metal mesh will be exited faster out of the RF-ICP reactor, thereby minimizing further the back reaction toward CO_2. Without increased pumping speed inside the RF-ICP reactor the CO_2 flow will interact less with the metal mesh surface thereby making the metal mesh capsule become transparent inside the RF-ICP reactor.
Stainless steel mesh capsules show here also a catalytic effect in a RF-ICP plasma reactor. This confirms our previous interpretation, using the catalyst holder equipped with brass meshes, that the metal meshes increases the recombination reaction of atomic O into O_2, thereby reducing the back reaction of CO into CO_2.
FIG. 3b shows a picture of the stainless steel mesh capsule before and after the CO_2 plasma exposure. After plasma exposure the clear visible effect is observed that the metal oxide layer is changed (i.e. thickness of metal oxide layer has increased) when the CO_2 plasma has percolated through and has cruised over the metal mesh capsule. The CO_2 plasma only exposed the areas that were in direct contact with the plasma beam during the CO_2 splitting process. The sides and the bottom of the plasma exposed stainless steel mesh capsule were unaffected (see also FIG. 3b). The majority of CO_2 splitting takes place at the core of the plasma beam.
Based on the findings above we have performed an experiment to test if multiple metal mesh capsules in an RF-ICP reactor will give more increased CO_2 conversions.
Here the effect on the CO_2 splitting performance is tested when the entire RF-ICP plasma reactor (except the centre part) is filled with both brass and stainless steel mesh capsules (see FIG S5). The centre part of the RF-ICP reactor (where the RF coil is located) does not contain metal mesh, because these capsules will interfere and prevent the ignition into CO_2 plasma. The result of FIG. S5a tell us that too much mesh capsules inside the RF-ICP reactor take up too much space in order to let the CO_2 gas be ignited into CO_2 plasma. The CO_2 splitting via multiple metal mesh capsules shows that the conversion only drops with 3-5%. Still even with

multiple metal mesh capsules there is still a catalytic effect that enables a higher conversion compared to the results of the empty RF-ICP reactor.
FIG. S5b shows how the CO_2 plasma interacts with multiple mesh capsules inside the RF-ICP reactor. At most locations in the RF-ICP reactor the CO_2 plasma is percolating through and cruising over some mesh capsule. Only at the entrance side of the RF-ICP reactor there is some difficulty to keep the CO_2 gas ignited as plasma.
After plasma exposure the surface colour of both stainless steel and brass mesh capsules have changed. A similar effect has also been observed with Cu based mesh capsules.

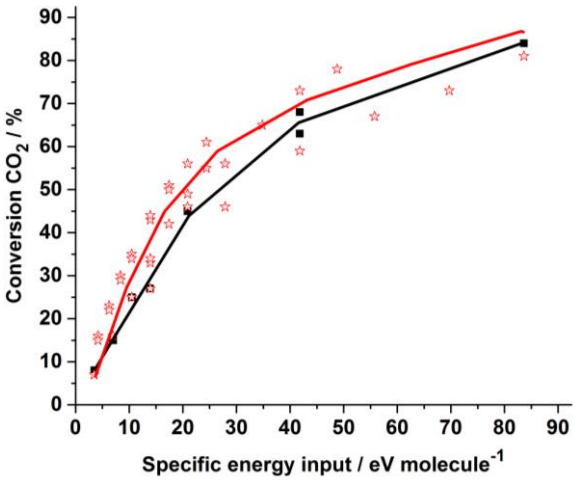

FIG. 4 The conversion as function of the specific energy input plotted from data originating from CO_2 splitting in an empty plasma reactor (black cubes) versus the data originating from CO_2 splitting with a metal mesh inside the plasma reactor (red stars). The curved black and red lines are guides for the eyes.

FIG 4. shows a clear distinction in how the conversion CO_2 trend line increases upon use of a metal mesh during CO_2 splitting inside an RF-ICP reactor compared to the CO_2 splitting process via an empty reactor.

3. SEM analysis of metal meshes before and after plasma driven CO_2 splitting

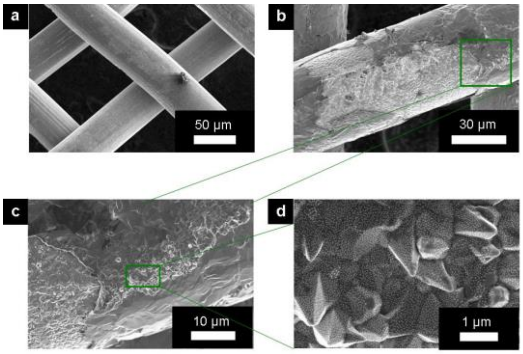

FIG. 5(a) SEM image of a Cu mesh not exposed to CO_2 plasma
(b-d) SEM images of a Cu mesh exposed to CO_2 plasma. The zoomed-in SEM images shows an area affected by 200 sccm CO_2 plasma.

FIG. 5a and 5b shows clearly how surface modification has occurred on the CO_2 plasma exposed Cu mesh. FIG. 5b shows us from the zoomed-in SEM image that the plasma exposed surface areas have become rough. The roughed Cu oxide area contains sharp angled shaped crystal structures.
CO_2 plasma generated by RF-ICP allows metals (brass, stainless steel, cupper) meshes to become catalysts. Thereby demonstrating the catalytic effect that it stimulates the recombination reaction of atomic O into O_2. This is an important discovery, because it means that non-thermal plasma is not only affecting the properties of CO_2 through vibrational activation. It means that RF driven plasma can change the properties of simple, cheap bulk metals and turn them into a new class/type of catalyst with specific catalytic properties that is not correlated with amount of metal meshes used during the CO_2 splitting process.

4. XPS analysis of metal meshes before and after plasma driven CO_2 splitting

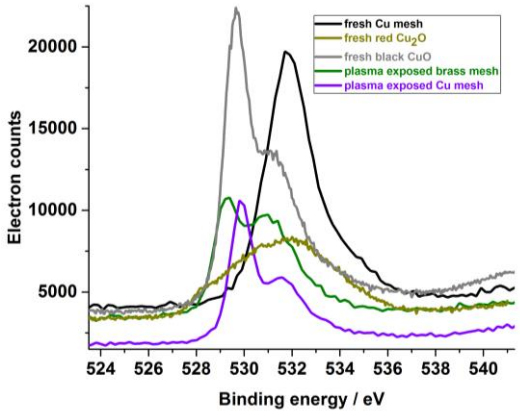

FIG. 6 XPS spectra of oxygen about fresh versus plasma exposed metal meshes. Curves are labelled A to E from top to bottom.

FIG. 6 shows in the O 1s spectrum that the plasma exposed metal meshes show a shift toward 530 eV, indicating that the presence of metal oxides have increased. The XPS spectra taken of sample D shows similar appearance with sample B, indicating that the plasma exposed Cu mesh presumable contains mostly CuO.
The difference in mass of the plasma exposed metal mesh versus the fresh metal mesh is about 0.002 till 0.003 gram.
FIG. S6 shows the XPS spectra of carbon about fresh versus plasma exposed metal meshes. The plasma exposed metal meshes show a lower intensity of carbon compared to the fresh metal meshes. Possibly carbonates on the metal meshes are removed by the CO_2 plasma. The decrease of the amount of carbon also shows than in the CO_2 dissociation no carbon is formed, that is deposited on metals in the reactor.
FIG. S7 shows Cu 2p XPS spectra of copper. Especially for a Cu mesh exposed by plasma there is a change in the type of Cu oxide. The fresh Cu mesh show peaks of mixed CuO and Cu_2O. When these Cu meshes are exposed to CO_2 plasma, the mix of both CuO and Cu_2O shifts more toward binding energies comparable to CuO. The dark surface colour of the plasma exposed Cu meshes confirm with the surface colour of fresh CuO.
XPS also indicates that the amount of carbon (i.e. carbonate) deposited on the surface has decreased due to the exposure with CO_2 plasma. The O_2 peak in the XPS spectra shows that the presence of O_2 slightly decreases and shift toward the binding energies of metal oxides below 531 eV. Focused Cu 2p XPS spectra reveals that the fresh metal meshes contain a mix of Cu_2O (932.5 eV), CuO (933.6 eV), $CuCO_3$ (935 eV) and $Cu(OH)_2$ (935.1 eV). When the metal meshes are exposed to CO_2 plasma a change and shift of Cu oxide peaks is observed toward the presence of mostly Cu_2O and/or CuO with sometimes some Cu visible.

5. XRD analysis of metal mesh exposed to thermal oxidation, thermal CO_2 exposure and plasma driven CO_2 splitting

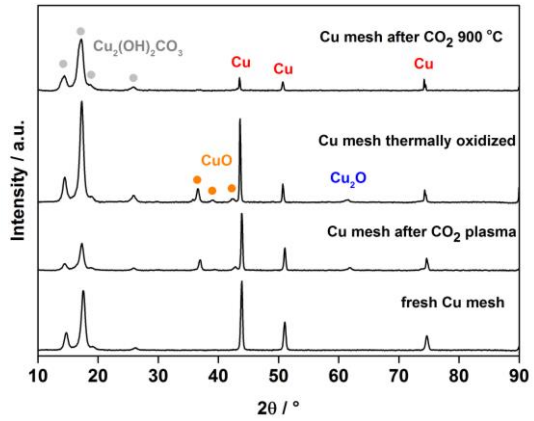

FIG. 7 XRD analyses of a fresh Cu mesh, Cu mesh exposed to 200 sccm CO_2 plasma (stepwise increase of power from 0 - 350 W), thermally oxidized Cu mesh and a Cu mesh exposed to thermal heated CO_2.

XRD analysis of a Cu mesh exposed to CO_2 plasma (see FIG. 7) confirms that the change in surface colour is related to the oxidation of the metal meshes in plasma.

From the results can be concluded that CO_2 splitting according to reaction 1 does not take place in thermal catalytic reactor at temperatures of 900 °C and a partial CO_2 pressure of > 2000 Pa. Via RF-ICP reactor, the conversion of CO_2 (reaction (1)), can be tuned by the feed flow, RF frequency, pressure, specific energy and input power.
The yield of CO can be significantly increased through the use of a metal mesh inside the RF-ICP reactor.
The CO_2 splitting driven by RF-ICP is here carried out through the presence and interaction of plasma. Plasma enables the dissociation of CO_2 through the presence of excited molecules. Theoretical analysis has indicated that vibrationally excited CO_2 will allow increased dissociation on metal surfaces i.e. like Ni [47, 48].
CO_2 splitting through thermal catalytic processes has never resulted into CO_2 conversion by dissociation [37, 47- 49]. Cu acts only as catalyst when methanol synthesis [15] is carried out under thermal-catalytic conditions.
We observe significant dissociation of CO_2 in the RF-ICP reactor, with or without catalyst. This must be due to plasma action. We observe a strong dependence between conversion and energy efficiency on plasma conditions, see FIG S4, 2 and 3. However, plotting both quantities as a function of the SEI more or less linear scaling is observed. This means that the conversion scales with the amount of energy introduced into the plasma per molecule flowing through the plasma channel.
A linear scaling with incident power or reactor pressure is not observed. An increase in the conversion with frequency has not been observed before. An increase in conversion with

increasing frequency is seen when comparing RF and microwave heating. Microwave heating is observed to be higher under similar conditions [32-34].
The presence of a metal mesh raises the CO yield about10% (i.e. absolute yield of CO). The relative increase of CO yield is around 20%. Several reasons can describe this effect.
The specifications of the plasma can be altered through the interaction with a metallic material. But observation of the plasma shows no change of the plasma beam intensity, colour or flow behaviour. This means that on the surface of the metal mesh a reaction occurs that initiates higher CO_2 conversions.
At a first sight the metal mesh appears to behave as an oxygen scavenger. From literature is well known that the recombination reaction of $CO + O + M \Rightarrow CO_2$ is detrimental for the CO_2 conversion. Here, the reactive O-atoms from the CO_2 splitting could be absorbed onto the metal mesh. This will increase the CO_2 conversion and the back reaction toward CO_2 will be reduced. As a consequence, the mass of the metal mesh should increase, but this is not happening here. XPS analysis of these plasma exposed metal meshes tells us that both carbon and oxygen are removed. In addition, SEM images of the plasma exposed metal meshes reveal that the surface of the metal mesh has undergo changes to the surface. These surface changes appear the same as thermal oxidation of Cu [45, 46]. These findings tell us that no oxygen will be taken up on these metal meshes due to these surface restructuring.
A second explanation to describe the CO yield increasing effect of these metal meshes in RF-ICP is that on the surface takes place the catalytic dissociation of CO_2. CO_2 can dissociate through interaction with vibrationally and translationally exited molecules on the metal surface [47, 48]. The origin of this interaction would take place within the potential energy surfaces for CO_2 – metal interactions. Here, the metal will become oxidized while the potential energy surface between the CO_2 and the metal will possess only a small barrier adjacent to the vibrational coordinate which in turn can accomplish the dissociation of CO_2 [47]. The O-atoms of the CO_2 will attach to the metal surface and thereby discard the remaining CO molecule. These interactions are possible based on theoretical and experimental studies via clean metal surfaces.
A similar process is the direct adsorption of free O-atoms at the surface of the mesh. This process will also cause an increase of the oxygen atom coverage on the surface. While in-diffusion of O-atoms is here limited [45], the adsorption of O-atoms will eventually give recombinative desorption. As a result O_2 molecules will be ejected from the metal mesh..
The reaction can be both a Langmuir-Hischelwood type or an Eley-Rideal reaction. Recently it was demonstrated that N-atoms created in a plasma are very efficient in removing O-atoms from a Ru surface [50].
While the molecules will be dissociated by the plasma, the reaction rate of dissociation of O_2 (i.e. reaction 4) is less than the dissociation of CO_2 (i.e. reaction 2) under the presence of a third body. This will enable to keep obstructing the back reaction to CO_2. This tells us that the metal mesh behaves as a catalyst that focus to favour the molecular recombination of atomic oxygen. As a result the coverage of oxygen on the surface of a metal mesh remains low and that corresponds with our XPS, XRD and SEM analyses where a oxide can be grown on a metal surface despite losing oxygen atoms inside the metal.
It is clear that not all plasma based species will be in contact with the metal mesh catalyst, because of limitations of the mean free path (i.e. < 0.1 mm). This means that diffusion is restricted aside the flow direction. Optimization in the flow and the design of the catalytic metal mesh will be required to increase further the CO yield.
Finally, in a other study was mentioned that bringing a metal mesh in contact with plasma would lead to sputtering effects where a metal films is deposited onto the quartz walls of the reactor [18]. From our experiences with metal meshes in RF-ICP this seems improbable.

With RF-ICP we observe a very sharp commencement of CO formation, while through a sputtering process a certain induction time is wanted to form up and complete a catalytic film in the reactor.

IV. CONCLUSION

CO_2 splitting (i.e. dissociation of CO_2 into CO) is activated by RF-ICP. The yield of CO in an empty RF-ICP reactor can be significantly increased through multiple ways.
By doubling the RF power frequency from 13.56 MHz to 27.12 MHz, an increase of CO yield is obtained of at least 10%.
Through tuning the CO_2 flow in an empty RF-ICP reactor, very high CO yield can be obtained (near 85% at 50 sccm CO_2). The increase in CO yield is not linearly related with the decrease in energy efficiency. While the energy efficiency of RF-ICP can be further improved, present plunges of renewable electricity cost favor the use of plasma conversion in general. Especially the easy switching of RF-ICP makes it suitable to store abundant electricity spikes quickly into CO as high-valuable chemical energy compound.
The most important way to increase the CO yield is through the discovery of catalytically driven recombination of atomic O's into O_2 by metal meshes in a RF-ICP reactor. This opens the way to toward new CO_2 splitting processes where the back reaction of CO to CO_2 is further reduced by means of a bulk material that gains catalytic properties through RF-ICP.

Supplementary materials:

In the supplementary materials is given an image of the used catalyst holder. We show additional information about the effects of the RF frequency on CO_2 splitting. Furthermore is shown the effects of plasma pretreatment on the reactor wall before CO_2 splitting. We show also the effect of tuning the CO_2 flow during on CO_2 splitting. Further we show the effect of multiple mesh capsules during CO_2 splitting. Finally, is shown additional XPS spectra of the meshes used before and after plasma driven CO_2 splitting.

V. ACKNOWLEDGEMENTS

Maria Ronda-Lloret is acknowledged for her support in analysing the metal mesh samples by SEM and XRD. Diyu Zhang, Dongping Wang and Qiang Huang are accredited for their discussions and support on CO_2 splitting experiments. Chuan-hui Liang is acknowledge for his support in analysing the metal mesh samples by XPS. Gadi Rothenberg and N. Raveendran Shiju are accredited for their scientific discussions on CO_2 splitting and catalytic processes.
This work has the support of the National Natural Science Foundation of China (Grant No. 51561135013 and 21603202). We thank the Netherlands Scientific Organisation (NWO) for the grant "Developing novel catalytic materials for converting CO2, methane and ethane to high-value chemicals in a hybrid plasma-catalytic reactor" (China.15.119).

1. J. Zhang, V. Haribal, F. Li, Perovskite nanocomposites as effective CO_2-splitting agents in a cyclic redox scheme, Sci. Adv. 2017,3, e1701184 (1-8)

2. Maria Tou, Ronald Michalsky, and Aldo Steinfeld, Solar-Driven Thermochemical Splitting of CO2 and In Situ Separation of CO and O2 across a Ceria Redox Membrane Reactor, Joule, 2018, 1, 19-23

3. Q. Jiang, Z. Chen, J. Tong, M. Yang, Z. Jiang and C. Li, Catalytic Function of IrOx in the Two-Step Thermochemical CO2‑Splitting Reaction at High Temperatures, ACS Catal. 2016, 6, 1172−1180

4. Snoeckx, R.; Bogaerts, A., Plasma Technology - a Novel Solution for CO2 Conversion? Chem. Soc. Rev. 2017, 46, 5805-5863.

5. J. D. Shakun, P. U. Clark, F. He, S. A. Marcott, A. C. Mix, Z. Y. Liu, B. Otto-Bliesner, A. Schmittner and E. Bard, Global warming preceded by increasing carbon dioxide concentrations during the last deglaciation, Nature 484, 2012, 49-54.

6. T. L. Frolicher, E.M. Fischer and N. Gruber, Marine heatwaves under global warming, Nature, 560, 2018, 360-364.

7. J.R. Malcolm, C.R. Liu, R.P. Neilson, L. Hansen and L. Hannah, Global warming and extinctions of endemic species from biodiversity hotspots, Conservation Biology, 20, 2006, 538-548.

8. I. A. Grant Wilson, IA Grant and P. Styring, Why Synthetic Fuels Are Necessary in Future Energy Systems, Frontiers in Energy Research, 5, 2017.

9. Detz, R. J.; Reek, J. N. H.; van der Zwaan, B. C. C., The future of solar fuels: when could they become competitive? Energy Environ. Sci. 2018, 11 (7), 1653-1669.

10. Birdja, Y. Y.; Perez-Gallent, E.; Figueiredo, M. C.; Gottle, A. J.; Calle-Vallejo, F.; Koper, M. T. M., Advances and challenges in understanding the electrocatalytic conversion of carbon dioxide to fuels. Nat. Energy 2019, 4 (9), 732-745.

11. Bogaerts, A.; Neyts, E. C., Plasma Technology: An Emerging Technology for Energy Storage. ACS Energy Lett. 2018, 3 (4), 1013-1027.

12. Bogaerts, A.; Kozak, T.; van Laer, K.; Snoeckx, R., Plasma-based conversion of CO2: current status and future challenges. Faraday Discuss. 2015, 183, 217-232.

13. Tao, X. M.; Bai, M. G.; Li, X. A.; Long, H. L.; Shang, S. Y.; Yin, Y. X.; Dai, X. Y., CH4-CO2 reforming by plasma - challenges and opportunities. Prog. Energy Combust. Sci. 2011, 37 (2), 113-124.

14. Chung, W. C.; Chang, M. B., Review of catalysis and plasma performance on dry reforming of CH4 and possible synergistic effects. Renew. Sust. Energ. Rev. 2016, 62, 13-31.

15. Wang, L.; Yi, Y. H.; Wu, C. F.; Guo, H. C.; Tu, X., One-Step Reforming of CO2 and CH4 into High-Value Liquid Chemicals and Fuels at Room Temperature by Plasma-Driven Catalysis. Angew. Chem.-Int. Edit. 2017, 56 (44), 13679-13683.

16. Bongers, W.; Bouwmeester, H.; Wolf, B.; Peeters, F.; Welzel, S.; van den Bekerom, D.; den Harder, N.; Goede, A.; Graswinckel, M.; Groen, P. W.; Kopecki, J.; Leins, M.; van Rooij, G.; Schulz, A.; Walker, M.; van de Sanden, R., Plasma-driven dissociation of CO2 for fuel synthesis. Plasma Process. Polym. 2017, 14 (6), 8.

17. van Rooij, G. J.; van den Bekerom, D. C. M.; den Harder, N.; Minea, T.; Berden, G.; Bongers, W. A.; Engeln, R.; Graswinckel, M. F.; Zoethout, E.; de Sandena, M., Taming microwave plasma to beat thermodynamics in CO2 dissociation. Faraday Discuss. 2015, 183, 233-248.

18. Shah, J.; Wang, W. Z.; Bogaerts, A.; Carreon, M. L., Ammonia Synthesis by Radio Frequency Plasma Catalysis: Revealing the Underlying Mechanisms. ACS Appl. Energ. Mater. 2018, 1 (9), 4824-4839.

19. Uyama, H.; Nakamura, T.; Tanaka, S.; Matsumoto, O., CATALYTIC EFFECT OF IRON WIRES ON THE SYNTHESES OF AMMONIA AND HYDRAZINE IN A RADIOFREQUENCY DISCHARGE. Plasma Chemistry and Plasma Processing 1993, 13 (1), 117-131.

20. Tanaka, S.; Uyama, H.; Matsumoto, O., SYNERGISTIC EFFECTS OF CATALYSTS AND PLASMAS ON THE SYNTHESIS OF AMMONIA AND HYDRAZINE. Plasma Chemistry and Plasma Processing 1994, 14 (4), 491-504.

21. Shah, J.; Wu, T.; Lucero, J.; Carreon, M. A.; Carreon, M. L., Nonthermal Plasma Synthesis of Ammonia over Ni-MOF-74. ACS Sustain. Chem. Eng. 2019, 7 (1), 377-383.

22. Peng, P.; Schiappacasse, C.; Zhou, N.; Addy, M.; Cheng, Y. L.; Zhang, Y. N.; Ding, K.; Wang, Y. P.; Chen, P.; Ruan, R., Sustainable Non-Thermal Plasma-Assisted Nitrogen Fixation-Synergistic Catalysis. ChemSusChem 2019, 12 (16), 3702-3712.

23. Patel, H.; Sharma, R. K.; Kyriakou, V.; Pandiyan, A.; Welzel, S.; van de Sanden, M. C. M.; Tsampas, M. N., Plasma-Activated Electrolysis for Cogeneration of Nitric Oxide and Hydrogen from Water and Nitrogen. ACS Energy Lett. 2019, 4 (9), 2091-2095.

24. Carreon, M. L., Plasma catalytic ammonia synthesis: state of the art and future directions. Journal of Physics D-Applied Physics 2019, 52 (48), 25.

25. Iwamoto, M.; Akiyama, M.; Aihara, K.; Deguchi, T., Ammonia Synthesis on Wool-Like Au, Pt, Pd, Ag, or Cu Electrode Catalysts in Nonthermal Atmospheric-Pressure Plasma of N-2 and H-2. ACS Catal. 2017, 7 (10), 6924-6929.

26. Aihara, K.; Akiyama, M.; Deguchi, T.; Tanaka, M.; Hagiwara, R.; Iwamoto, M., Remarkable catalysis of a wool-like copper electrode for NH3 synthesis from N-2 and H-2 in non-thermal atmospheric plasma. Chem. Commun. 2016, 52 (93), 13560-13563.

27. Bryony Ashford, Xin Tu*, Non-thermal plasma technology for the conversion of CO2, Current Opinion in Green and Sustainable Chemistry , 2017, 3, 45-49

28. T. Butterworth, R. Elder and R. Allen, Effects of particle size on CO2 reduction and discharge characteristics in a packed bed plasma reactor, Chemical Engineering Journal, 2016, 293, 55–67

29. Erik C. Neyts, Kostya (Ken) Ostrikov, Mahendra K. Sunkara, and Annemie Bogaerts. Plasma Catalysis: Synergistic Effects at the Nanoscale, Chemical Reviews 2015, 115, 13408−13446.

30. Amin Jafarzadeh,* Kristof M. Bal, Annemie Bogaerts, and Erik C. Neyts. Activation of CO_2 on Copper Surfaces: The Synergy between Electric Field, Surface Morphology, and Excess Electrons, Journal of Physical Chemistry C, 2020, 124, 6747-6755

31. Z. Li, T. Yang, S. Yuan, Y. Yin, E. J. Devid, Q. Huang, D. Auerbach, A. W. Kleyn, Boudouard Reaction Driven by Thermal Plasma for Efficient CO_2 Conversion and Energy Storage, Journal of Energy Chemistry 2020, 45, 128.

32. L. F. Spencer and A. D. Gallimore. Efficiency of CO2 Dissociation in a Radio-Frequency Discharge Plasma Chem Plasma Process, 2011, 31, 79-89

33. Spencer, L. F.; Gallimore, A. D., CO2 dissociation in an atmospheric pressure plasma/catalyst system: a study of efficiency. Plasma Sources Science & Technology 2013, 22 (1).

34. Q. Huang, D. Y. Zhang, D. P. Wang, K. Z. Liu, A. W. Kleyn, Journal of Physics D-Applied Physics 2017, 50, 6;

35. S. Poulston, P. M. Parlett, P. Stone and M. Bowker, Surface Oxidation and Reduction of CuO and CuzO Studied Using XPS and XAES, Surface and Interface analysis, 1996, 24, 811-820

36. S. Funk, B. Hokkanen, J. Wang, U. Burghaus, G. Bozzolo and J. E. Garcés , Adsorption dynamics of CO2 on Cu(110): A molecular beam study, Surface Science 600 (2006) 583–590

37. U. Burghaus , Surface science perspective of carbon dioxide chemistry-Adsorption kinetics and dynamics of CO2 on selected model surfaces, Catalysis Today, 2009, 148, 212-220

38. U. Burghaus, Surface chemistry of CO2-Adsorption of carbon dioxide on clean surfaces at ultrahigh vacuum, Progress in Surface Science, 2014, 89, 161-217

39. Yao, Y. X.; Shushkov, P.; Miller, T. F.; Giapis, K. P., Direct dioxygen evolution in collisions of carbon dioxide with surfaces (vol 10, 2294, 2019). Nature Communications 2019, 10, 1.

40. D. Y. Zhang, Q. Huang, E. J. Devid, E. Schuler, N. R. Shiju, G. Rothenberg, G. van Rooij, R. L. Yang, K. Z. Liu, A. W. Kleyn, J. Phys. Chem. C 2018, 122, 19338-19347.

41. R. L. Yang, D. Y. Zhang, K. W. Zhu, H. L. Zhou, X. Q. Ye, A. W. Kleyn, Y. Hu, Q. Huang, Acta Phys.-Chim. Sin. 2019, 35, 292-298.

42. S. V. T. Nguyen, J. E. Foster, A. D. Gallimore, Operating a radio-frequency plasma source on water vapor, Rev. Sci. Instrum. 2009, 80, 083503 (1-8).

43. J. Perez-Ramirez, R. J. Berger, G. Mul, F. Kapteijn, J. A. Moulijn, Catal. Today 2000, 60, 93–109

44. N. Madaan, R. Haufe, N. R. Shiju, G. Rothenberg, Top. Catal. 2014, 57, 1400–1406

45. J. C. Yang, B. Kolasa, J. M. Gibson, and M. Yeadon, Self-limiting oxidation of copper, Appl. Phys. Lett., 1998, 73, 2841-2843

46. C. Gattinoni, A. Michaelides, Atomistic details of oxide surfaces and surface oxidation: the example of copper and its oxides, Surface Science Reports, 2015, 70, 424–447.

47. B. Jiang, and H. Guo, Communication: Enhanced dissociative chemisorption of CO2 via vibrational excitation, Journal of Chemical Physics, 2016, 144(9), 5.

48. Zhou, X. Y.; Kolb, B.; Luo, X.; Guo, H.; Jiang, B., Ab lnitio Molecular Dynamics Study of Dissociative Chemisorption and Scattering of CO2 on Ni(100): Reactivity, Energy Transfer, Steering Dynamics, and Lattice Effects. J. Phys. Chem. C 2017, 121 (10), 5594-5602.

49. C. L. Kao, A. Carlsson and R. J. Madix, The adsorption dynamics of molecular carbon dioxide on Pt(111) and Pd(111), Surface Science., 2002, 497(1-3), 356-372.

50. Zaharia, T.; Kleyn, A. W.; Gleeson, M. A., Eley-Rideal Reactions with N Atoms at Ru(0001): Formation of NO and N-2. *Phys. Rev. Lett.* **2014,** *113* (5).

Supplementary materials

Conversion of CO_2 by non-thermal inductively-coupled plasma catalysis

Edwin Devid*[a], Maria Ronda-Lloret[b], Qiang Huang[a,c], Gadi Rothenberg[b], N. Raveendran Shiju[b], Aart Kleyn*[a]

[a] dr. E. J. Devid, dr. Q. Huang, Prof. dr. A. W. Kleyn
Center of Interface Dynamics for Sustainability
Institute of Materials, China Academy of Engineering Physics
596 Yinhe Road 7th section, Chengdu, Sichuan 610200, People's Republic of China
E-mail: ejdevid@outlook.com ; a.w.kleijn@contact.uva.nl

[b] M. Ronda-Lloret MSc., Prof. dr. G. Rothenberg, dr. N. Raveendran Shiju
Van 't Hoff Institute for Molecular Sciences
Faculty of Science, University of Amsterdam
P.O. Box 94157, 1090 GD Amsterdam, The Netherlands

[c] Dr. Q. Huang
School of Optoelectronic Engineering
Chongqing University of Posts and Telecommunications
Chongqing 400065, People's Republic of China

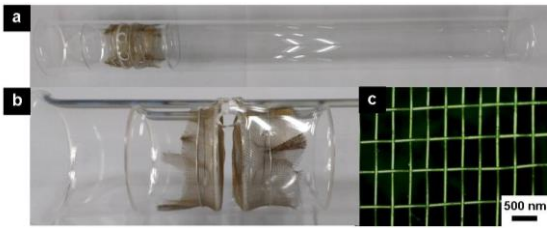

FIG. S1 (a) The catalyst holder, a component developed for our RF-ICP reactor to enable materials to interact fully with CO_2 plasma. Here the material inserted in the catalyst holder are two brass meshes. (b) A zoom-in image of the empty catalyst bed between the two meshes. (c) A microscope image of the dimensions of the brass mesh used for CO_2 splitting.

1. The effect of the RF frequency on CO_2 splitting

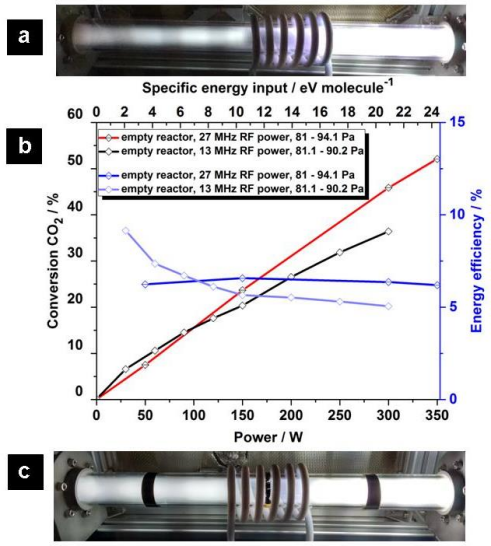

FIG. S2 (a) Image of 200 sccm CO_2 plasma at 300 W with at frequency of 13.56 MHz. The pressure in the RF-ICP reactor is 90.2 Pa and the CO_2 feed gas goes from the left to the right side.
(b) The CO_2 conversion and energy efficiency as function of the input power and SEI (Reaction conditions: 200 sccm CO_2).
(c) Image of 200 sccm CO_2 plasma at 300 W with at frequency of 27.12 MHz. The pressure in the RF-ICP reactor is 92.3 Pa and the CO_2 feed gas goes from the left to the right side.

2. Effect of pretreatment air plasma on reactor wall before CO_2 splitting

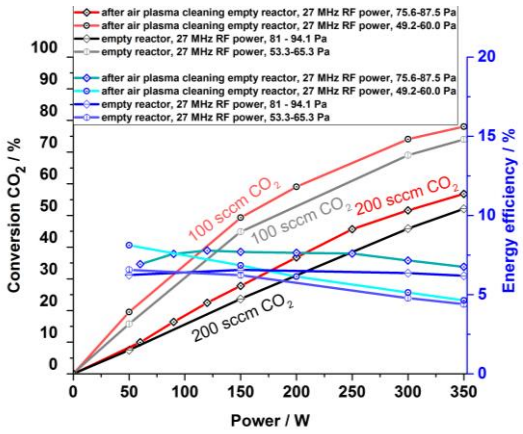

FIG. S3 The CO_2 conversion and energy efficiency as function of the input power. Reaction conditions: black lines display conversion at flow rates 100 and 200 sccm CO_2, the red lines display conversion at flow rate 100 and 200 sccm CO_2 after pretreatment with air plasma (200 sccm air) at 200 W for 45 min and then for 15 min at 300 W.

3. The effect of tuning the CO_2 flow on the CO_2 splitting process

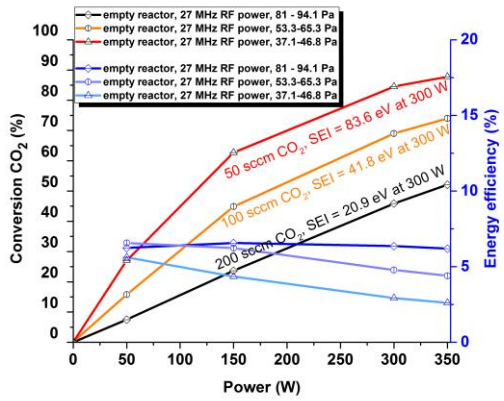

FIG. S4 The CO_2 conversion and energy efficiency as function of the input power. Reaction conditions: black line displays conversion at flow rate 200 sccm CO_2, orange line displays conversion at flow rate 100 sccm CO_2 and red line displays conversion at flow rate 50 sccm CO_2.

4. Effect of multiple brass and stainless steel mesh capsules in the reactor for CO_2 splitting

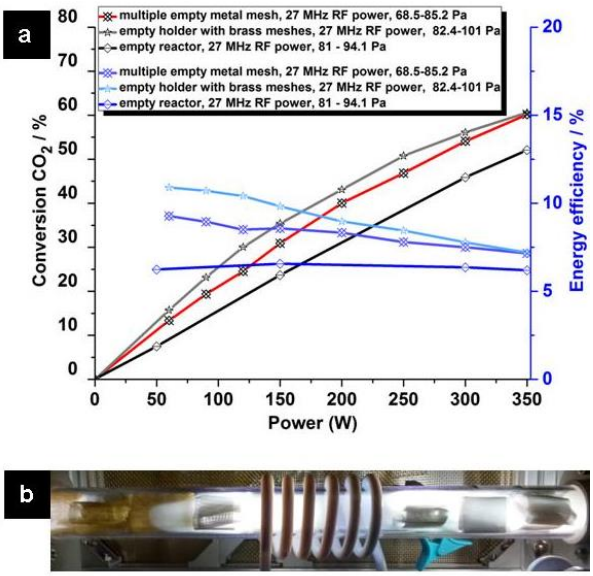

FIG. S5 (a) The CO_2 conversion and energy efficiency as function of the input power. Black line is reference conversion of an empty RF-ICP reactor. Red line is the conversion obtained via multiple stainless steel and brass mesh capsules.
(b). An image of the RF-ICP plasma reactor filled with four stainless steel and three brass mesh capsules exposed to CO_2 plasma (at 250 W and pressure of 79.2 Pa).
Reaction conditions: 200 sccm CO_2 and in FIG. S5b the CO_2 plasma flows from left side to the right side. For the experiment with using multiple metal mesh capsules an additional second vacuum pump (located at the side toward the QMS) is used to lower a bit the starting pressure (with 5 till 7 Pa) before the plasma driven CO_2 splitting is started.

5. XPS analyses of metal meshes before and after plasma driven CO_2 splitting

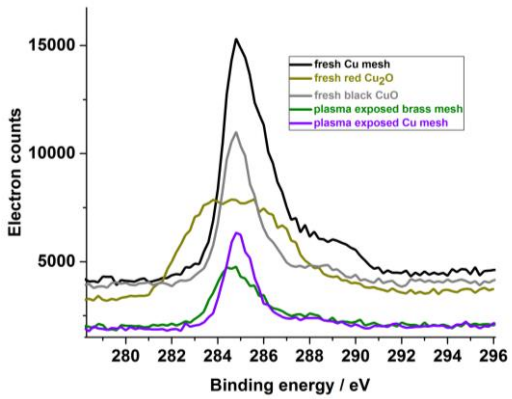

FIG. S6 XPS spectra of carbon about fresh versus plasma exposed metal meshes

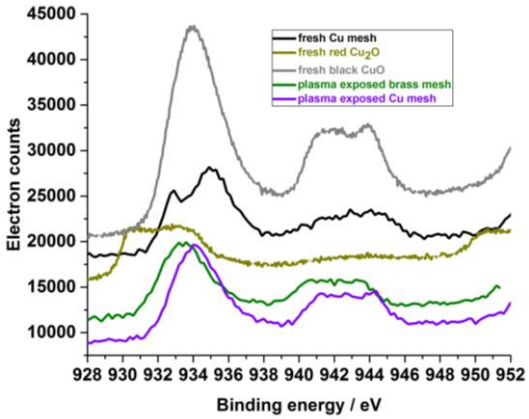

FIG. S7 XPS spectra of cupper about fresh versus plasma exposed metal meshes